ELSEVIER

Thermochimica Acta 291 (1997) 171–177

thermochimica acta

Kinetic parameters obtained from TPR data for α-Fe_2O_3 and Au/α-Fe_2O_3 systems

G. Munteanu[a,*], L. Ilieva[b], D. Andreeva[b]

[a] *Institute of Physical Chemistry I.G. Murgulescu of the Romanian Academy, 202 Splaiul Independentei, Bucharest 77208, Romania*
[b] *Institute of Catalysis, Bulgarian Academy of Sciences, Sofia 1113, Bulgaria*

Received 26 June 1996; received in revised form 27 September 1996; accepted 8 October 1996

Abstract

Kinetic parameters were evaluated by simulation of experimental temperature-programmed reduction spectra of α-Fe_2O_3 and Au/α-Fe_2O_3 systems. It was established that gold influences only the first reduction step $Fe_2O_3 \rightarrow Fe_3O_4$, the pre-exponential value for Au/α-Fe_2O_3 being substantially higher than that for α-Fe_2O_3. The presence of hydroxyl coverage entails decreasing of the activation energy of this step. © 1997 Elsevier Science B.V.

Keywords: Au/α-Fe_2O_3; *Kinetic parameters; Temperature-programmed reduction*

1. Introduction

Studies on Au/α-Fe_2O_3 catalysts in water-gas shift reaction (WGSR) have revealed a high catalytic activity of these catalysts at low temperatures [1,2]. Using temperature-programmed reduction (TPR) and temperature-programmed desorption (TPD) techniques it has been shown that in the presence of gold, α-Fe_2O_3 is reduced to magnetite which is a catalytically active phase at considerably lower temperatures than non-promoted α-Fe_2O_3 [3]. A higher coverage of hydroxyl groups on the surface is also favoured. This finding agrees with a proposed WGSR mechanism which involves both a surface OH group in the formation of the intermediate and a redox $Fe^{+2} \leftrightarrow Fe^{+3}$ transition in a magnetite matrix [2].

It is of interest to compare the TPR spectra of the α-Fe_2O_3 system with those of Au/α-Fe_2O_3 system not only qualitatively – a routine encountered in many papers – but to estimate the respective kinetic parameters as well. This could allow one to draw some conclusions about the effect of added gold and the hydroxyl surface coverage on the α-$Fe_2O_3 \rightarrow Fe_3O_4$ reduction process, which is of substantial importance for the study of the WGSR mechanism on iron catalysts.

2. Experimental

Two samples, α-Fe_2O_3 and Au/α-Fe_2O_3, denoted by A and B respectively, were investigated. They were prepared by coprecipitation according to a procedure described in detail earlier [2,3]. Sample α-Fe_2O_3, previously dehydroxylated at 823 K in a stream of moisture- and oxygen-free helium and sample Au/α-

---

*Corresponding author. Tel.: 00401 312 11 47; fax: 00401 312 11 47; e-mail:gmunteanu@roimar.imar.ro.

PII S0040-6031(96)03097-3

Fe_2O_3, also dehydroxylated under the same conditions, are denoted by Aδ and Bδ respectively. All the TPR measurements were carried out by means of an apparatus described in [4], under the following conditions: a hydrogen-argon mixture (10% H_2) at a flow rate of 24 ml min^{-1}; a temperature rise of 15 K min^{-1}; 0.01 g of sample.

3. Principles

The kinetic parameters, characteristic to the processes in which the peaks on the TPR profiles originate, were evaluated by simulations of the TPR experiments [5]. We proceeded in this way to determine these parameters, taking account of all experimental conditions used in our measurements. Moreover, our opinion is that this is the only procedure that allows an evaluation of the kinetic parameters when TPR peaks overlap.

The previous procedure used for TPR experiment simulations has been adapted to the present conditions taking account of the following:

1. Fig. 1 shows the experimental TPR profiles for all four samples investigated. One may notice that each profile has two maxima, the first peak having a shoulder on the side of lower temperatures, in case of sample A;
2. In case of samples B and Bδ the two peaks are isolated, the ratio between their peak areas being 1 : 8; and
3. Analyzing these two samples, we have noticed [3] that after the first peak, located at 623 K, they consist only of Fe_3O_4, but after the second, located at ~900 K, they consist only of metallic iron.

Taking into account the foregoing facts, we considered that the two hydrogen consumptions, corresponding to the two TPR peaks, are due to the following two processes:the first peak:

$$3Fe_2O_3 + H_2 \rightarrow 2Fe_3O_4 + H_2O \qquad (1)$$

and the second peak:

$$2(Fe_3O_4 + 4H_2 \rightarrow 4Fe + 4H_2O) \qquad (2)$$

The reactions described by Eqs. (1) and (2) have different molecularities and orders. Consequently, it was not possible to compare the kinetic parameters characteristic of the two processes: the pre-exponential factors could not be compared because they have different dimensions and a comparison of the values of the activation energies alone is usually irrelevant.

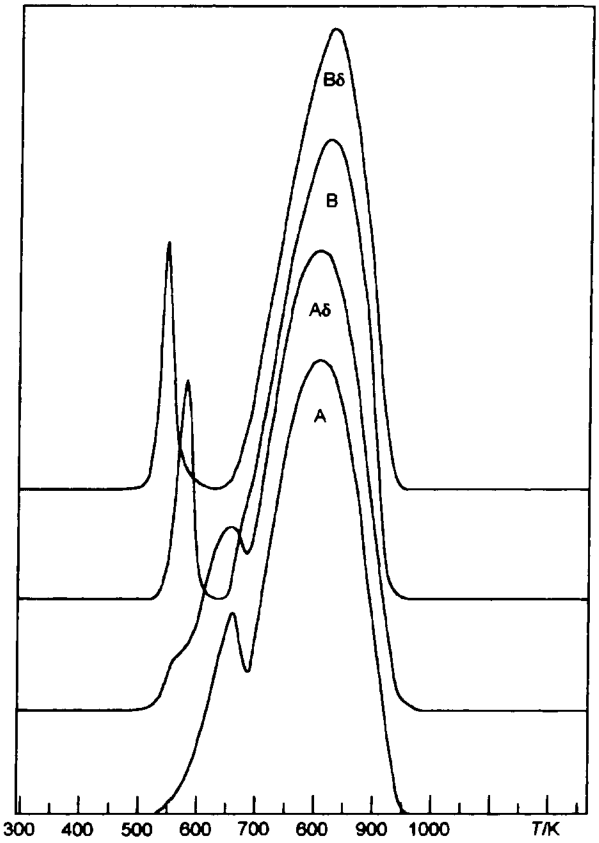

Fig. 1. Experimental TPR profiles: A – fresh α-Fe_2O_3, Aδ – dehydroxylated α-Fe_2O_3, B – fresh Au/α-Fe_2O_3, and Bδ – dehydroxylated Au/α-Fe_2O_3.

To compare the kinetic parameters, it is necessary to reduce the two processes to reactions with identical orders and molecularities. To do this we have to take into account the fact that, during the reduction of a certain oxide, each hydrogen molecule reacts with a surface oxygen atom:

$$\{O\}_S + H_2 \rightarrow \{\square\}_S + H_2O \qquad (3)$$

where $\{O\}_S$ implies a surface oxygen atom and $\{\square\}_S$ an anionic vacancy that results from such a reaction. Consequently, we can consider, formally at least, that the two processes described by Eqs. (1) and (2), take place according to the reactions:

$$Fe_2O_3 + H_2 \rightarrow 2FeO + H_2O \quad (4)$$

$$2(FeO + Fe_2O_3 \rightarrow Fe_3O_4) \quad (5)$$

and, respectively,

$$Fe_3O_4 + H_2 \rightarrow 3FeO + H_2O \quad (6)$$

$$3(FeO + H_2 \rightarrow Fe + H_2O) \quad (7)$$

In this way the processes described by Eqs. (1) and (2) are replaced by the three hydrogen consuming processes – described by Eqs. (4),(6) and (7) – that have the same orders and molecularities as the elementary processes described by Eq. (3). In these three processes the ratio of hydrogen consumptions is 1 : 2 : 6.

To make the processes described by Eqs. (4) and (5) equivalent to that described by Eq. (1) it is enough to assume that the rate of the reaction in Eq. (5) is much higher than that of the reaction in Eq. (4). Thus, the reaction in Eq. (4) is the rate-limiting step and, consequently, the kinetic parameters characteristic of the reaction in Eq. (4) may be regarded as characteristic of the reaction in Eq. (1). Whether the two processes take place or not according to Eqs. (4)–(7) is not essential. Only the three processes which consume hydrogen, have the same orders and molecularities and thus the values of the pre-exponential factors and of their activation energies can be compared.

In the following, we consider that during a TPR experiment in which one of the four iron oxide samples is reduced, the following processes take place:

$$Fe_2O_3 \xrightarrow{k_1} Fe_3O_4 \xrightarrow{k_2} FeO \xrightarrow{k_3} Fe$$

the rate constants k_1, k_2, k_3 being characteristic of the processes described by Eqs. (4),(6) and (7), respectively.

Taking account of the fact that any of the three reactions may be a second-order reaction, the reaction rate, for any of them, may be written as:

$$v_i = k_{0_i} x_i y \exp(-E_i/RT) \quad (8)$$

where i=1, 2, and 3, and x_i the concentration of the oxide species i (i=1 for Fe_2O_3, 2 for Fe_3O_4, and 3 for FeO), y the hydrogen concentration in the reaction space, k_{0_i} the pre-exponential factor and E_i the activation energy. Using a procedure described before [5,6], we obtained the following form for the reaction rates:

$$v_i = \frac{2D_0 y^{\mathrm{in}}}{V_r \frac{p}{p_0} \frac{T_0}{T} + \frac{2D_0}{k_{0_i} x_i} \exp(E_i/RT)}, \; i = 1,2,3 \quad (9)$$

where V_r is the reaction volume, p and p_0 the pressure in the reaction space and the normal pressure, respectively, T and T_0 the temperature in the reaction space and the normal temperature, respectively, D_0 the flow rate of the reducing mixture measured in normal conditions of pressure and temperature (24 ml min^{-1} in our case), y^{in} the hydrogen concentration at the inlet of the reactor, the other notations having the usual meaning. In our case the reaction volume was 0.2 ml and the pressure in the reaction space was equal to the normal pressure.

The concentrations of the three types of iron oxide, as functions of temperature, were computed by numerical integration of Eq. (9) using the Runge–Kutta method of fourth order [7]. The TPR curves were simulated by computing the hydrogen consumption, Δy, by Eq. (10):

$$D\Delta y = vV_r \quad (10)$$

where D is the flow rate of the reducing mixture in the reaction space and $v = v_1 + v_2 + v_3$ the rate of hydrogen consumption in reactions in Eqs. (4),(6) and (7).

The kinetic parameters characteristic of the three processes were evaluated by curve fitting. In our simulations, we assumed that the pre-exponential factors k_{0_2} and k_{0_3} are equal. We also assumed that $E_2 < E_3$, because the process described by Eq. (6) precedes the one described by Eq. (7).

4. Results and discussion

The TPR experimental data [3] shows that a shoulder appears on the low-temperature side of the first peak (Fig. 1, curve A) only in the case of α-Fe_2O_3. We assigned this shoulder to hydroxylated iron oxide. After dehydroxylation this shoulder disappeared (Fig. 1, curve Aδ).

Samples Au/α-Fe_2O_3 and dehydroxylated Au/α-Fe_2O_3 exhibit only two maxima (Fig. 1, curves B and Bδ). One can also notice that the second peak, which results from a two-step reduction of magnetite to metallic iron is nearly the same in all the samples studied.

In case of the Au/α-Fe_2O_3 sample, the reduction of hematite to magnetite takes place at lower temperatures than that of α-Fe_2O_3 ($T^{B}_{1,\max} = 553$ K and $T^{A}_{1,\max} = 700$ K, respectively). Regarding the same reduction step: the Au/α-Fe_2O_3 exhibited a higher reducibility than the dehydroxylated Au/α-Fe_2O_3 ($T^{B}_{1,\max} = 553$ K and $T^{B\delta}_{1,\max} = 588$ K, respectively).

The kinetic parameters which characterize these processes were evaluated by simulation for each TPR profile. The computed TPR profiles are shown in Figs. 2 and 3, and the values of the kinetic parameters are presented in Table 1. Differences are

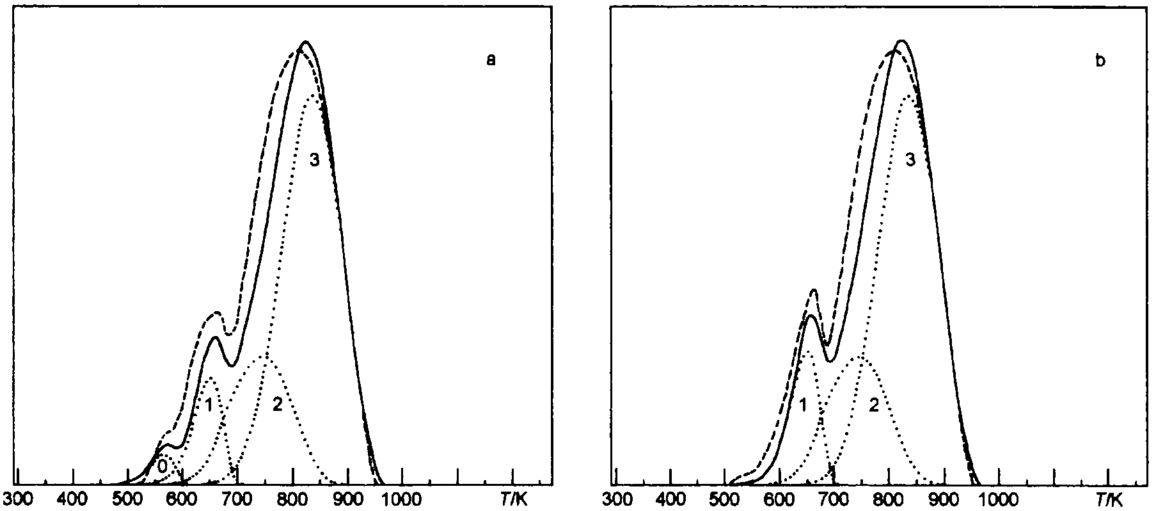

Fig. 2. Experimental (broken line) and simulated (continuous line) TPR spectra of (a) fresh and (b) dehydroxylated α-Fe_2O_3. Dotted curves denote hydrogen consumption corresponding to individual reduction processes: (0) – hydroxylated α-$Fe_2O_3 \rightarrow Fe_3O_4$; (1) – dehydroxylated α-$Fe_2O_3 \rightarrow Fe_3O_4$; (2) – $Fe_3O_4 \rightarrow FeO$; and (4) – $FeO \rightarrow Fe$.

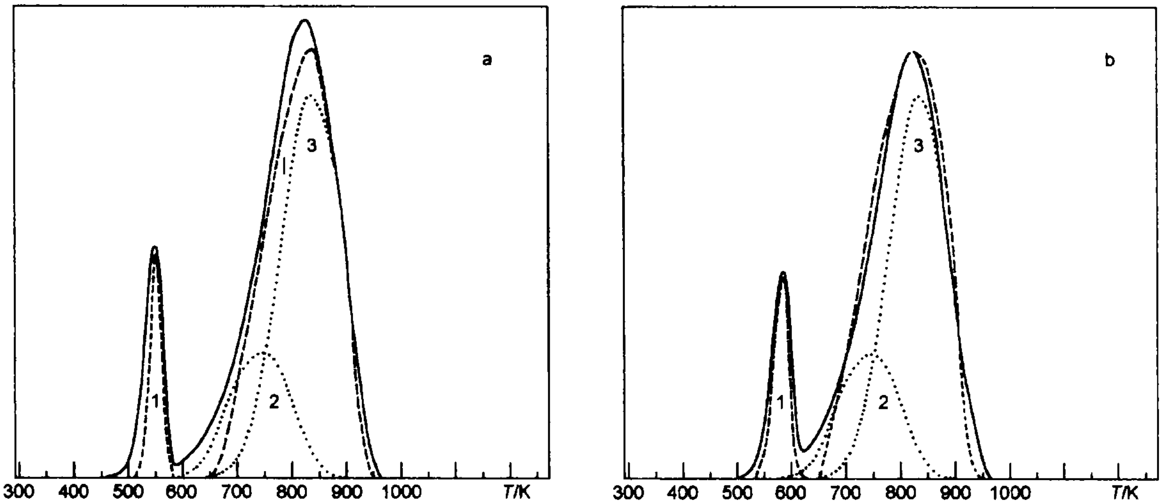

Fig. 3. Experimental (broken line) and simulated (continuous line) TPR spectra of (a) fresh and (b) dehydroxylated Au/α-Fe_2O_3. Dotted curves denote hydrogen consumption corresponding to individual reduction processes: (1) – α-$Fe_2O_3 \rightarrow Fe_3O_4$; (2) – $Fe_3O_4 \rightarrow FeO$; and (4) – $FeO \rightarrow Fe$.

Table 1
Kinetic parameters

Sample	$Fe_2O_3 \rightarrow Fe_3O_4$		$Fe_3O_4 \rightarrow FeO$		$FeO \rightarrow Fe$	
	$k_{0_1}/(m^3\ mol^{-1}\ s^{-1})$	$E_1/(kJ\ mol^{-1})$	$k_{0_2}/(m^3\ mol^{-1}\ s^{-1})$	$E_2/(kJ\ mol^{-1})$	$k_{0_3}/(m^3\ mol^{-1}\ s^{-1})$	$E_3/(kJ\ mol^{-1})$
A	2.4×10^8	139.2	6×10^2	77.3	6×10^2	85.7
Aδ	2.4×10^8	139.2	6×10^2	77.3	6×10^2	85.7
B	5.4×10^{12}	172.2	6×10^2	77.3	6×10^2	85.7
Bδ	5.4×10^{12}	162.2	6×10^2	77.3	6×10^2	85.7

observed in the values of the kinetic parameters which are specific to the reduction of hematite to magnetite. Concerning further reduction steps, all the values are similar in all investigated samples. It is seen from Table 1 that the value of activation energy of $Fe_2O_3 \rightarrow Fe_3O_4$ transition is higher than the values of the two subsequent reduction steps: $Fe_3O_4 \rightarrow FeO \rightarrow Fe$. This was somewhat unexpected but very close data on the activation energy of Fe_2O_3/SiO_2 samples, 155.9 and 77.3 kJ mol^{-1}, have been reported for the $Fe_2O_3 \rightarrow Fe_3O_4$ and $Fe_3O_4 \rightarrow Fe$ transitions, respectively [8]. Shinokawabe et al. [9] have also reported a higher value of the activation energy of hematite reduction to magnetite than that of the reduction of magnetite to metallic iron in a study on Fe_2O_3 prepared from $Fe(OH)(CH_3COO)_2$. Other authors [10] have reported data on the activation energies of the same transitions upon reduction of small Fe_2O_3 particles in a moisture-rich reducing mixture. In this case, the two TPR peaks are separated, the value of the activation energy of the first transition being lower than that of the second one. In case of a dry reducing mixture the present authors followed Kissinger's method which allows one to determine only the activation energy of the $Fe_3O_4 \rightarrow Fe$ transition that is dominant in the doublet of overlapping TPR peaks.

However, in order to compare the two processes it is also necessary to evaluate the rate constants, their temperature dependence and the values of the pre-exponentials. It is seen from Table 1 that the pre-exponential values of the $Fe_3O_4 \rightarrow FeO \rightarrow Fe$ transitions are considerably lower than those of the $Fe_2O_3 \rightarrow Fe_3O_4$ transition.

Table 2 lists the ratios between the rate constants of the consecutive reduction steps of α-Fe_2O_3 and Au/α-Fe_2O_3 and their temperature dependence. For the two samples investigated, the ratio between the rate constants of the $Fe_3O_4 \rightarrow FeO$ and the $FeO \rightarrow Fe$ reduction steps decreased from 5.0 to 3.0 when the temperature was increased from 723 to 923 K, respectively. This means that, in this temperature range, the rate constants of the two processes are nearly the same. This fact explains why the two corresponding TPR peaks overlap. We could therefore state that in fact the reduction of Fe_3O_4 takes place, in only one step, directly to metallic iron. This conclusion would be in agreement with the remark of Unmuth et al. [8] that, at the temperature of Fe_3O_4 reduction to metallic iron, according to the phase diagrams of the Fe–O system [11], the oxide form FeO cannot occur.

In the case of α-Fe_2O_3, the ratio of the rate constants of the $Fe_2O_3 \rightarrow Fe_3O_4$ and the $Fe_3O_4 \rightarrow FeO$ reduction steps increased from only 0.27 to 14.0 when the temperature increased from 523 to 723 K. Even by the end of the former process, the difference between the two rate constants was not significant. Therefore the two peaks, corresponding to the two processes, over-

Table 2
Ratio of rate constants at various temperatures

Sample	$k_{0_1}\exp(-E_1/RT)/k_{0_2}\exp(-E_2/RT)$			$k_{0_3}\exp(-E_3/RT)/k_{0_2}\exp(-E_2/RT)$		
	523 K	623 K	723 K	723 K	823 K	923 K
α-Fe_2O_3	0.27	2.6		14 5.0	3.9	3.0
Au/α-Fe_2O_3	30	690		6700 5.0	3.9	3.0

lap (see Fig. 2). In the case of Au/α-Fe_2O_3 the same ratio increased from 30 to 6 700 over the 523–723 K temperature range. Here the rate constant of the first reduction step is much higher than the rate constant of the second reduction step, the two processes being separated (Fig. 3).

However, it should be noted that in order to simulate the TPR profile of α-Fe_2O_3 it did not suffice to take account only of the three processes mentioned here. A complementary process, which corresponds to the shoulder in the experimental TPR profile (Fig. 2a), was also considered. We assumed that this shoulder originates in the reduction of some hydroxylated iron oxide. The following values of the kinetic parameters, $k_0=2.4\times10^8$ m^3 mol^{-1} s^{-1} and $E=121.2$ kJ mol^{-1}, were used for this process.

Fig. 2(a) presents the peaks assigned to the individual hydrogen consumptions, which correspond to the four processes. By overlapping these individual peaks we obtained a TPR profile which fits quite well with the experimental peak.

In case of dehydroxylated α-Fe_2O_3, a simulation could be carried out based only on the three subsequent reduction steps (see Fig. 2b). During the simulation of the shoulder in the TPR spectrum of this system, utilization of the same value of the pre-exponential and of a value of the activation energy lower than the corresponding value of the first reduction step ($Fe_2O_3 \rightarrow Fe_3O_4$) proved to be consistent with the conclusion that the role of the hydroxyl groups is to diminish the activation energy of the process of hematite reduction to magnetite.

The effect of the hydroxyl coverage is obvious in the case of gold-containing iron oxide. After dehydroxylation the first TPR peak appeared at a higher temperature (i.e. at $T^{\mathrm{B}}_{1,\max} = 588\,\mathrm{K}$ with $T^{\mathrm{B}\delta}_{1,\max} = 553\mathrm{K}$, Fig. 3(a,b)). As can be seen in Table 1, the same value of the pre-exponential was used to simulate the first peak with hydroxylated and dehydroxylated Au/α-Fe_2O_3. However, the activation energy of the dehydroxylated Au/α-Fe_2O_3 was higher than that of the hydroxylated one, taking the values of 172.2 and 162.2 kJ mol^{-1}, respectively. This confirmed our conclusion concerning the influence of the hydroxyl coverage on the activation energy of the process of hematite reduction to magnetite.

Comparison of the kinetic parameters, which specify the $Fe_2O_3 \rightarrow Fe_3O_4$ transition in dehydroxylated α-Fe_2O_3 and Au/α-Fe_2O_3 (Table 1), shows that the introduction of gold leads to substantially higher values of the pre-exponential factor. The value of the activation energy of dehydroxylated α-Fe_2O_3 (139.2 kJ mol^{-1}) is lower than that of dehydroxylated Au/α-Fe_2O_3 (172.2 kJ mol^{-1}) irrespective of the considerably lower value of $T_{\max}$ of the first peak of the gold-containing sample. However, as already mentioned it is also necessary to compare the respective rate constants. At 523 K, the $k_{\mathrm{B}\delta}/k_{\mathrm{A}\delta}$ ratio is only 11.3 which means that the first reduction step of the two samples starts at comparable temperatures. However, at 623 and 723 K this ratio becomes 38.4 and 92.6, respectively. This indicates that on increasing the temperature, the rate constant of the first reduction step of the dehydroxylated Au/α-Fe_2O_3 becomes much higher than that of the dehydroxylated α-Fe_2O_3. These results explain well the TPR spectra obtained experimentally. The reduction of hematite to magnetite in the dehydroxylated gold-containing sample is completed at a temperature at which the first TPR peak of the dehydroxylated α-Fe_2O_3 has not reached its maximum yet. A conclusion can be drawn: the effect of gold as promoter is consistent with an increase in the rate constant of α-$Fe_2O_3 \rightarrow Fe_3O_4$ process, due to a considerable increase of the value of the pre-exponential factor.

Acknowledgements

The present work has been partially supported by the National Foundation for Scientific Research, Bulgaria, and the Ministry of Research and Technology, Romania.

References

[1] D. Andreeva, V. Idakiev, T. Tabakova and A. Andreev, J. Catal. 158 (1996) 354.

[2] D. Andreeva, V. Idakiev, T. Tabakova, A. Andreev, R. Giovanoli, Appl. Catalalysis A: General (1995) in press.

[3] L. Ilieva, D. Andreeva, A. Andreev, Thermochim. Acta, submitted.

[4] N.K. Kotsev and D.M. Shopov, J. Catal. 22 (1971) 297.

[5] G. Munteanu and M. Craiu, React. Kinet. Catal. Lett. 50 (1993) 49.

[6] D.A.M. Monti and A. Baiker, J. Catal. 83 (1983) 323.

[7] N. Bachvalov, Numerical Methods, Mir, Moscow, p. 434.
[8] E.E. Unmuth, L.H. Schwartz and J.B. Butt, J. Catal. 61 (1980) 242.
[9] M. Shimokawabe, R. Furuichi and T. Ishii, Therm. Acta 28 (1979) 287.
[10] O.J. Wimmers, P. Arnoldy and J.A. Moulijn, J. Phys. Chem. 90 (1986) 1331.
[11] E.M. Levin, C.R. Robbins and H.F. McMurdle, Phase Diagrams for Ceramists, Am. Ceramic Soc., Columbus OH, USA (1964) p. 5.